Molecular Crystals and Liquid Crystals

Publication details, including instructions for authors and subscription information:
http://www.tandfonline.com/loi/gmcl20

Dielectric, Thermally Stimulated Discharge Current, Pyroelectric and Surface Morphology of Pmma Thin Films Prepared by Isothermal Immersion

B. Shekar [a], Moonkyong Na [a], Jiyeon Lee [a] & Shi-Woo Rhee [a]

[a] System on Chip Process Research Center, Department of Chemical Engineering, Pohang University of Science and Technology, Pohang, Korea

Version of record first published: 18 Oct 2010

To cite this article: B. Shekar, Moonkyong Na, Jiyeon Lee & Shi-Woo Rhee (2004): Dielectric, Thermally Stimulated Discharge Current, Pyroelectric and Surface Morphology of Pmma Thin Films Prepared by Isothermal Immersion, Molecular Crystals and Liquid Crystals, 424:1, 43-53

To link to this article: http://dx.doi.org/10.1080/15421400490505866

Mol. Cryst. Liq. Cryst., Vol. 424, pp. 43–53, 2004

ISSN: 1542-1406 print/1563-5287 online
DOI: 10.1080/15421400490505866

Taylor & Francis
Taylor & Francis Group

DIELECTRIC, THERMALLY STIMULATED DISCHARGE CURRENT, PYROELECTRIC AND SURFACE MORPHOLOGY OF PMMA THIN FILMS PREPARED BY ISOTHERMAL IMMERSION

B. Chandar Shekar, MoonKyong Na, Jiyeon Lee, and Shi-Woo Rhee
System on Chip Process Research Center, Department of Chemical Engineering, Pohang University of Science and Technology, Pohang, 790-784, Korea

Metal–Insulator–Metal structure was used to investigate the dielectric, thermally stimulated discharge current (TSDC) and pyroelectric behavior of poly methyl methacrylate (PMMA) thin films prepared by isothermal immersion method. The surface morphology and the structure of the above said films were studied by using atomic force microscopy (AFM) and X-ray diffraction (XRD) respectively. The XRD spectrum of as grown and films annealed at 513 K indicated the amorphous nature. No pits and dendritic features were observed from the AFM spectrum. The only important topographic features observed is the hillocks of about 10–12 nm large with a peak to valley vertical distance of about 0.5–1 nm. Both as grown and films annealed at 513 K showed very smooth surface and amorphous nature. From the TSDC spectrum activation energy (E), capture cross-section (σ), escape frequency (ν) and relaxation time (τ) were calculated. The observed amorphous phase, low loss, dielectric and thermal behavior imply the feasibility of utilizing PMMA thin films as gate dielectric insulator layer in organic thin film transistors (OTFTs), which can find application in flat panel display.

Keywords: dielectric; morphology and dipolar-reorientation; pyroelectric; PMMA; TSDC

1. INTRODUCTION

Poly methyl methacrylate (PMMA) is one of the potential vinyl polymer. The structure of the PMMA macromolecule is linear with respect to the main carbon chain. The dipole moment of PMMA is associated with

Received 1 October 2003; accepted 11 February 2004.

Address correspondence to Shi-Woo Rhee, Department of Chemical Engineering, POSTECH, Pohang, 790-784, South Korea. Tel.: 054-279-8614, Fax: 054-279-8619, E-mail: chandar@postech.ac.kr

the ester group $COOCH_3$ and the orientation of this group in the electric field while the thermo electrets formed is responsible for the appearance of a hetero-charge [1,2]. It is used as thick transparent windows; large aquariums; paints; a small amount of PMMA dissolved oils and fluids can be used to operate machines up to 173 K; PMMA coated along with inorganic materials such as SiO_2 and TiO_2 (to increase hardness and to reduce surface reflections) is widely used for optical instruments such as optical lenses in camera, glasses, optical fiber and endoscopes; PMMA thin films having very smooth surface and low surface roughness can be used as dielectric insulator layer in organic thin film transistors (OTFTs); and as skin permeation enhancer after corona charged. The stability of dipole orientation and space charge storage of PMMA is directly related to the effect of drug skin permeation. So the studies of establishment of electret state, stability of dipole orientation and ability of space charge storage of PMMA for electret–drug transdermal delivery system are of great importance in basic study [3–5].

2. EXPERIMENTAL

PMMA ($M_w = 96,700$, purchased from Aldrich) was used as received without further purification. Glass micro slides and p-type silicon wafers were used as substrates. Glass micro slides were cleaned by ultrasonic agitation and vapor degreasing methods where as the p-type silicon wafers were degreased with organic solvents such as trichloroethylene (TEC) and acetone followed by a rinse in deionized water (DI), boiled in nitric acid (HNO_3) for 10 min, dipped in dilute hydrofluoric (HF) for 10 sec and finally rinsed in DI water. X-ray diffract meter (XRD) and Atomic Force Microscope (AFM) were used to investigate the structure and morphology of the PMMA thin films. Dielectric, TSDC and pyroelectric behavior were studied by using sandwich configurations of MIM structures. In the MIM structure pure aluminum (99.99, Balzers) was thermally evaporated under a vacuum of 10^{-5} Torr to form the base metal electrode, the middle polymer insulator layer was formed by depositing poly methyl methacrylate by isothermal immersion method and finally aluminum was again evaporated over the polymer layer to form the top electrode. In the present investigation anisole, benzene, chloroform and acetone were used as solvents to prepare PMMA films. Dielectric properties were studied by measuring capacitance (C) and loss ($\tan\delta$) using Hewlett-Packard LCR meter for the frequency range (10 kHz–10 MHz). TSDC and pyroelectric studies were carried out for PMMA film of thickness 500 nm for the polarizing temperatures (T_p) of 305 and 333 K under different polarizing fields ($E_p = 6$, 10 and 18 MV/m) for the temperature range of 303 K to 365 K. The films were

annealed in a vacuum of 10^{-3} Torr by keeping them at 400 K for one hour under a bias of 2 volts. Then the samples were polarized for 1 h by keeping them in a specially constructed jig. The jig was placed in an electro statically shielded vessel which was evacuated to a vacuum of 10^{-3} Torr. The films were heated indirectly at a constant heating rate. To study the TSDC and pyroelectricity the annealed films were cooled from high temperature to room temperature in the presence of the electric field. At room temperature, the samples were kept short circuited for 5 min to remove any surface charges present and then the samples were linearly heated up to 365 K with a uniform heating rate and the currents were measured. An EA815 electrometer amplifier was used to measure the depolarization currents.

3. RESULTS AND DISCUSSION

3.1. Structure and Surface Morphology

The surface morphologies of thin films can be characterized by using many methods such as scanning electron microscopy (SEM), transmission electron microscopy (TEM) and atomic force microscopy (AFM), etc. AFM has become a powerful technique and has been widely used to measure the surface morphology of polymer films because of its high surface sensitivity and simplicity of sample preparation [6,7]. The Figures from Figure 1a to Figure 1e show the 3D atomic force micrograph (AFM) image of as grown and annealed PMMA films of various thicknesses in the nanometer range deposited on silicon substrate. No pits and dendritic features were observed in the topographical image of the samples studied. The only important topographic feature observed is the hillocks of about 10–12 nm large with a peak to valley vertical distance of about 0.5–1 nm. The surface smoothness was found to be improved by annealing the films at 513 K for 30 min. The observed features of the as grown and films annealed at 513 K indicated the amorphous nature of the PMMA films. Table 1 shows the roughness analysis values of as grown and annealed PMMA films of various thicknesses. The surface roughness was found to be very low for as grown and annealed PMMA films. X-ray diffraction spectrum of as grown PMMA films deposited from the solution of PMMA dissolved in different solvents such as chloroform, acetone, anisole and benzene are shown in Figure 2. The X-ray diffraction pattern indicates the amorphous nature with large diffraction maxima that decreases at large diffraction angles. The shape of the first main maximum indicates the ordered packing of the polymer chains. The intensity and shape of the second maxima are related to the effect of ordering inside the main chains. The observed broad humps in the XRD spectrum indicate the presence of crystallites of very low dimensions. The absence of any prominent peaks in the as grown

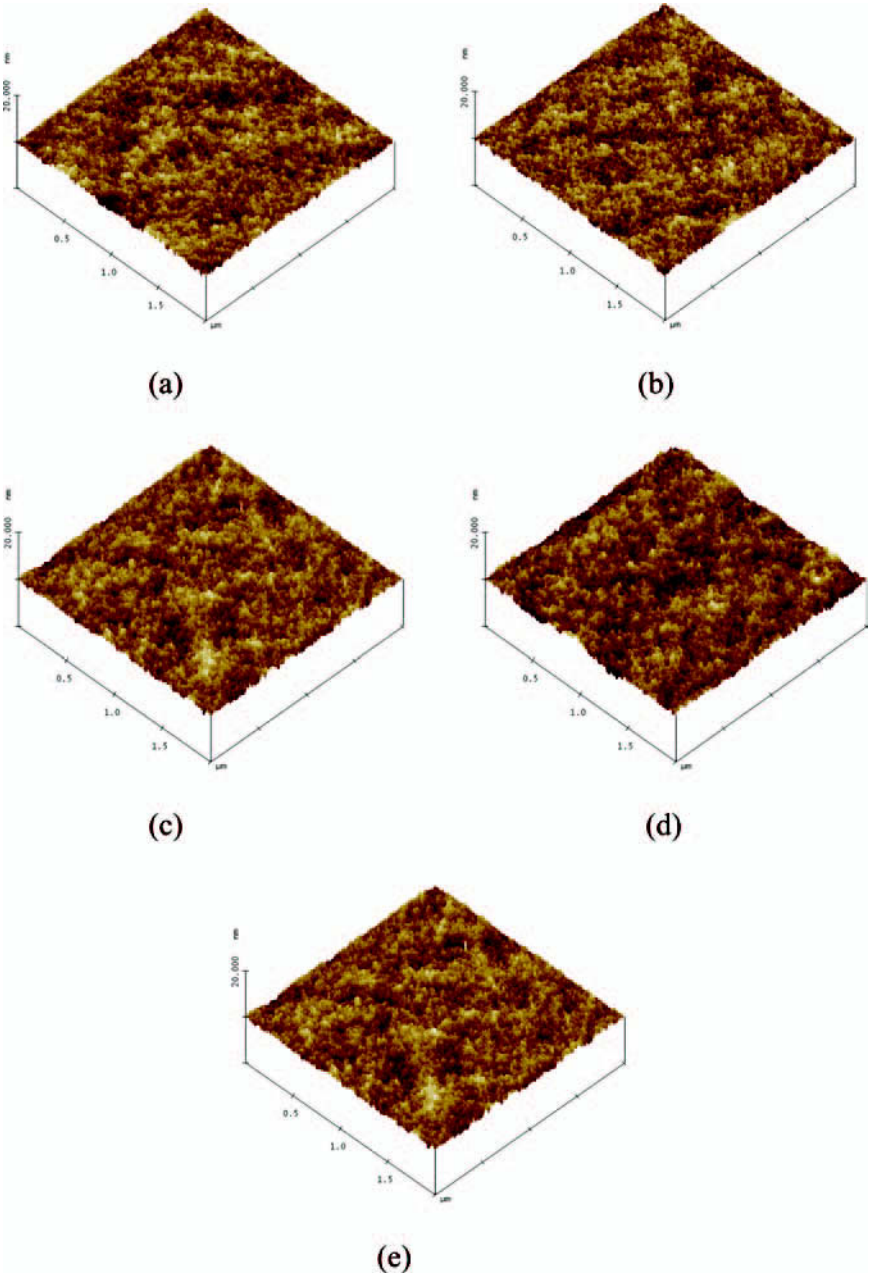

FIGURE 1 3D AFM of as grown PMMA of (a) 1800 Å, (b) 2070 Å, (c) 2375 Å, (d) 3515 Å, & (e) annealed PMMA of 3515 Å at 513 K.

TABLE 1 Roughness Analysis of PMMA Films

PMMA	Thickness (Å)	Surface area (μm)	Surface area difference	Mean roughness (Ra) (nm)	RMS Roughness (nm)
As grown	1800	4.006	0.154	0.252	0.317
	2070	4.007	0.167	0.234	0.293
	2370	4.005	0.115	0.264	0.332
	3515	4.000	0.162	0.276	0.335
Annealed at 513 K	3515	4.006	0.162	0.267	0.335

(Fig. 2) and annealed (Figure not shown) PMMA thin films indicates the predominantly amorphous nature of the films. The observed spectrum also indicated the absence of solvent molecules in the PMMA film. Table 2 shows the values of intensity, I/I_o and FWHM with D-spacing or the angle of incidence 2θ. The observed results indicate that the value of intensity, I/I_o and FWHM are not changing much with annealing the films at 513 K for 30 min.

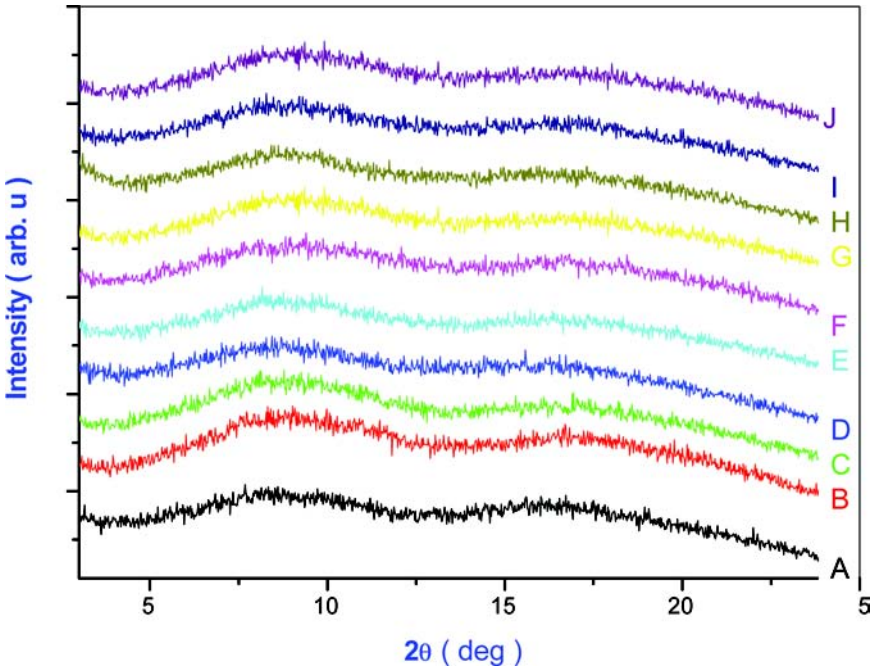

FIGURE 2 XRD of as grown PMMA film of thickness (A) 375 Å, (B) 1150 Å (C) 1800 Å, (D) 2065 Å, (E) 2300 Å, (F) 2375 Å, (G) 3370 Å, (H) 3415 Å, (I) 3515 Å & (J) 2070 Å.

TABLE 2 The Values of Intensity, I/I_o and FWHM for as Grown and Annealed Films

Film	2θ	D-spacing	Intensity	I/I_o	FWHM
(A) 3515 Å, as grown	9.68	9.1291	1275	96	0.28
	17.60	5.035	1044	78.6	0.14
(B) 3515 Å, annealed	9.46	9.3414	1327	99.1	0.28
at 513 K	16.48	5.3746	1112	83	0.26
(C) 2370 Å, as grown	9.74	9.0736	1371	96.7	0.26
	17.76	4.99	1124	79.3	0.18
(D) 2370 Å, annealed	9.5	9.3023	1315	96.7	0.22
at 513 K	17.6	5.035	1038	76.3	0.26
(E) 1800 Å, as grown	9.68	9.1291	1514	98.1	0.30
	17.44	5.0808	1152	74.6	0.22
(F) 1800 Å, annealed	9.68	9.1291	1218	98.8	0.28
at 513 K	17.6	5.035	1017	82.5	0.24

3.2. Dielectric Behavior

The purpose of the dielectric studies is to understand (a) the annealing behavior, (b) variation of capacitance with temperature and frequency, (c) variation of dielectric constant with temperature and frequency and (d) variation of dielectric loss with temperature and frequency. Generally the dielectric constant is calculated using the formula

$$C_i = \frac{\varepsilon_0 \varepsilon'}{d}$$

where $C_i, \varepsilon_0, \varepsilon', d$ are the capacitance per unit area of the gate insulator, the permittivity of free space, dielectric constant and the thickness of the insulator layer respectively. The variation of dielectric constant with temperature is different for polar and non-polar polymers. Dielectric constant is independent of temperature for non-polar polymers whereas for strong polar polymers dielectric constant increases with temperature. In the case of weakly polar polymers the dielectric constant decreases initially and then started increasing with temperature. The dielectric loss factor $(\varepsilon''(\omega))$ is calculated by using the loss value $(\tan\delta)$ and dielectric constant $(\varepsilon(\omega))$ value from the relation $\varepsilon(\omega) = \varepsilon''(\omega)/\tan\delta$. The saturation dipole polarization (P_s) or the persistent polarization (P_p) was determined by using the values $\varepsilon_s - \varepsilon_\infty$ and $\varepsilon(T_p) - \varepsilon(T_f)$, where ε_s is static dielectric constant, ε_∞ is optical dielectric constant, $\varepsilon(T_p)$ is static dielectric constant at the polarizing temperature T_p and $\varepsilon(T_f)$ is static dielectric constant at the final temperature T_f. The variation of dielectric constant with frequency for various temperatures is shown in the Figure 3. The observed decrease of dielectric constant with increasing frequency may be due to the tendency of induced dipoles in the PMMA to orient themselves in the direction of the

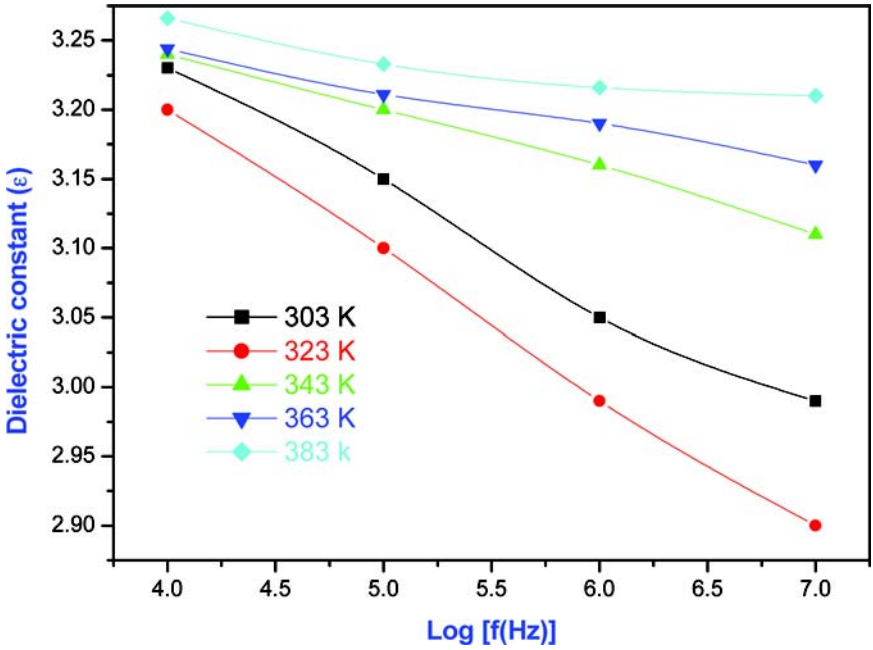

FIGURE 3 Dielectric constant *vs.* log f for PMMA film of 5000 Å thick for (■) 303 K, (●) 323 K, (▲) 343 K, (▼) 363 K & (◆) 383 K.

applied field [8]. The following equations can explain the observed dependence of dielectric constant ($\varepsilon(\omega)$) with frequency.

$$\varepsilon(\omega) = \frac{\varepsilon''(\omega)}{\tan\delta} = \frac{\varepsilon''(\omega)}{1/\omega RC + \omega RC}$$

where the value of $\varepsilon(\omega) \propto 1/\omega RC$ at low frequency and $\varepsilon(\omega) \propto \omega RC$ at high frequency. So when $\omega \to 0$, $\varepsilon''(\omega) \approx 0$ then $\varepsilon(\omega) = \varepsilon_s$ (static dielectric constant) and when $\omega \to \infty$, $\varepsilon''(\omega) \approx \infty$ then $\varepsilon(\omega) = \varepsilon_\infty$ (dielectric constant at optical frequencies). The observed dielectric spectrum (Fig. 3) shows the weak polar nature of the PMMA films. The increase of dielectric constant with temperature >323 K may be due to an increase of total polarization arising from dipoles and trapped charge carriers [9]. The variation of capacitance with frequency (Figure not included) showed that the capacitance decreases in the low frequency range and attains almost constant value in the high frequency range, which is the usual behavior observed in many polymer films. The decrease of capacitance (C) with increase of frequency may be attributed to the trapping-detrapping of charge carriers due to gap states density, increasing inability of the dipoles to orient

themselves in a rapidly varying electric field and slow release of charge carriers from relatively deep traps in the amorphous film [10]. The observed increase of capacitance above 323 K is partly due to the expansion of the lattice and partly due to the excitation of charge carriers present at the imperfection sites [11]. The variation of $\tan\delta$ with temperature for different frequencies (Figure not included) showed a loss peak near the glass transition temperature (T_g) of the PMMA films. The peak shifts to the high temperature side with an increase in frequency. The observed peak near 370 K is assigned to the α-transition (glass transition) and is due to the collective reorientation of the side groups with adjacent main chain segments $-C-CH_2-$. The peak is not symmetrical, with a broadening towards the lower temperatures, corresponding to the β' relaxation. The β' peak is attributed to the presence of heterotactic sequences in the conventional PMMA [1,2,12].

3.3. TSDC and Pyroelectric Behavior

TSDC is to study the polarization and depolarization behavior with respect to temperature and voltage. It gives vital information about the charge storage capacity of the material [1,5]. Depolarization current is given by relation $I = P(t)/\tau$, where $P(t)$ is the time dependent dipole polarization and τ is the relaxation time. TSDC spectrum shows that (Fig. 4) the magnitude of TSDC current increases with increase of polarizing temperature (T_p) and polarizing field (E_p). For the (T_p) of 305 K (Fig. 4) and 333 K (Figure not included), a peak was observed near 320 K for $E_p = 6$ MV/m for the temperature range studied. For $E_p = 18$ MV/m a peak was observed near 345 K for $T_p = 305$ K and around 324.5 K for $T_p = 333$ K. The observed peak is assigned to the β'-transition and it is attributed to the presence of heterotactic sequences [2]. Relaxation time (τ), activation energy (E), capture cross-section (σ) and escape frequency (v) were calculated by using the following relations.

$$\text{Relaxation time } (\tau) = \tau_0 \exp\left(-\frac{U}{kT}\right)$$

where $\tau_0 = kT_m 2/BU \exp(U/kT_m)$, $B = dT/dt$ is heating rate, k is the Boltzmann's constant, T_m is the peak temperature, U is the activation energy determined from semi log plot of $\ln I(T)$ *vs.* $1/T$.

$$\text{Capture cross section } (\sigma_n) = v/2.9 \times 10^{24}\, T_m^2 \text{ and}$$

$$\text{Escape frequency } (v) = \frac{3T'\beta}{2T_m(T_m - T')} \exp\left(\frac{U}{kT_m}\right)$$

where T' is the temperature at half maximum intensity on the low temperature side. The calculated values of activation energy (E) capture

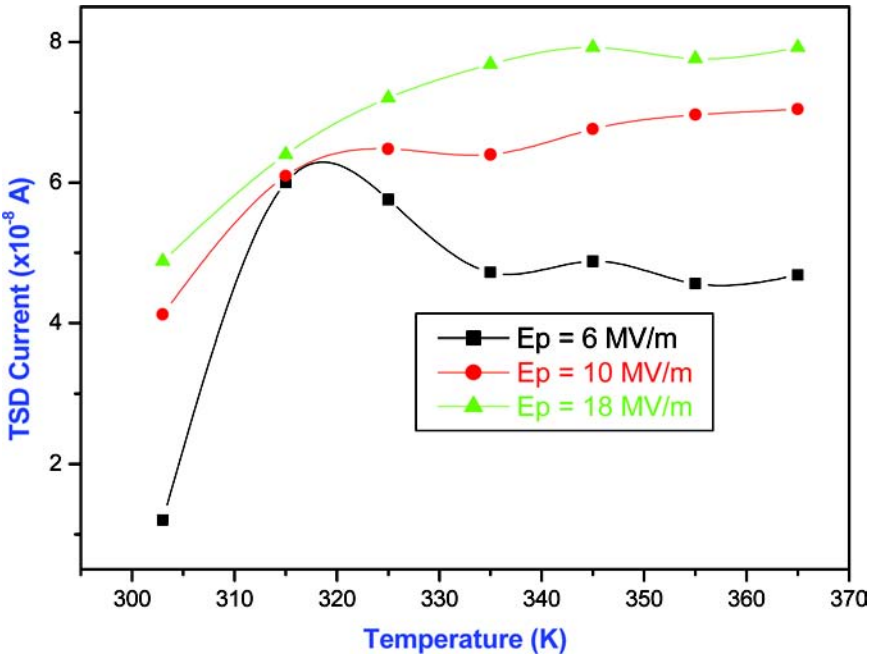

FIGURE 4 TSDC *vs.* temperature for PMMA film of 5000 Å thick polarized at 305 K for (■) Ep = 6 MV/m, (●) 10 MV/m & (▲) 18 MV/m.

cross-section (σ), escape frequency (ν) and relaxation time (τ) are given in the Table 3.

Pyroelectricity is a step extension of TSDC. After polarization the 1st cycle of depolarization gives TSDC (irreversible process) where as the 2nd and subsequent depolarization gives pyroelectricity (reversible process). Pyroelectricity gives the sustained depolarization behavior of

TABLE 3 Calculated Values of Activation Energy (E), Capture Cross-Section (σ), Escape Frequency (ν) and Relaxation Time (τ)

Polarizing temp. (K)	Polarizing field (MV/m)	Activation energy (eV)	Capture cross section 10^{-6} (m^2)
305	6	0.00121	5.12
	10	0.00129	
	18	0.00209	4.21
333	6	0.769	1.13
	10	0.701	
	18	0.041	

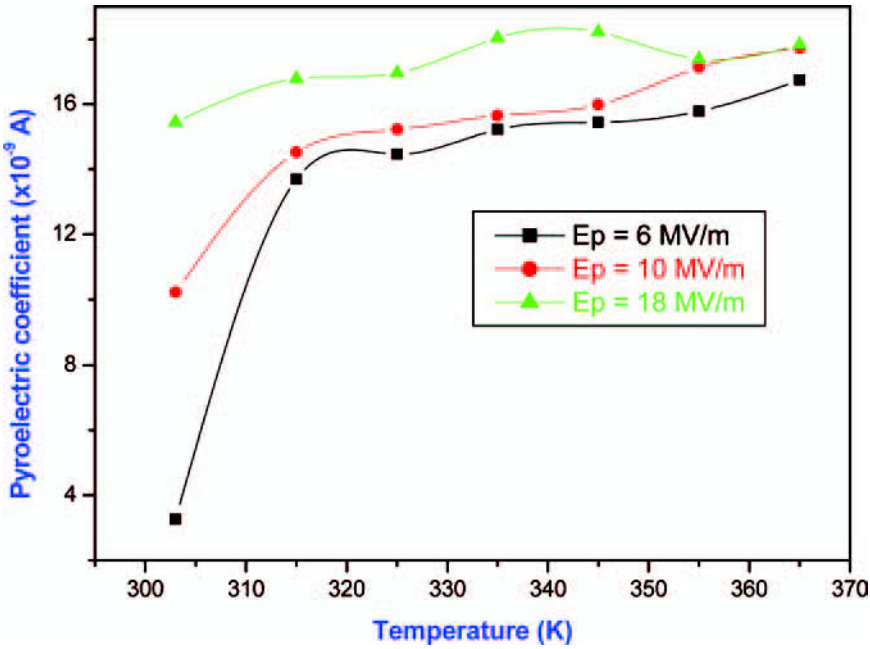

FIGURE 5 Pyroelectric coefficient *vs.* temperature for PMMA film of 5000 Å thick polarized at 305 K for (■) Ep = 6 MV/m, (●) 10 MV/m & (▲)18 MV/m.

the film. Pyroelectric coefficient is given by the relation $P = \pm I/AB$, where I is pyroelectric current, A is area of the film, $B = dT/dt$ is heating rate. P is positive for pyroelectric currents with same polarity as in TSDC and it is negative for pyroelectric currents with opposite polarity observed in TSDC. Figure 5 shows the pyroelectric spectrum observed for the polarizing temperature 305 K. For $T_p = 305$ K, as the polarizing field (E_p) increases the pyroelectric coefficient increases up to $E_p = 10$ MV/m and above this field the pyroelectric coefficient decreases with the increase of polarizing field. For $E_p = 18$ MV/m, a single peak was observed near 320 K. When T_p increased the pyroelectric coefficient showed complex behavior for all fields. For $E_p = 10$ and 18 MV/m, negative pyroelectric coefficient values were obtained at 333 K (Figure not included). The pyroelectric behavior observed may be due to the dipolar-reorientation process.

4. CONCLUSIONS

The absence of any prominent peaks in the XRD spectrum of as grown and annealed PMMA thin films indicated the predominantly amorphous nature

of the films. The XRD spectrum also indicated the absence of solvent molecules in the PMMA film. No pits and dendritic features were observed in the AFM topographical image of the samples studied. The only important topographic features observed is the hillocks of about 10–12 nm large with a peak to valley vertical distance of about 0.5–1 nm. The observed features of the as grown and films annealed at 513 K indicated the amorphous nature of the films studied. The observed TSDC and pyroelectric behavior may be attributed to the dipolar-reorientation process. The observed amorphous phase, dielectric behavior, thermal stability and low loss imply the possibility of utilizing PMMA thin films as a gate dielectric layer in OTFTs.

REFERENCES

[1] Van Turnhout, J. (1975). *Thermally Stimulated Discharge of Polymer Electrets*, Elsevier: Amsterdam.
[2] Mazur, K. (1997). *J. Phys. D: Appl. Phys*., *30*, 1383.
[3] Dimitrakopoulos, C. D., Furman, B. K., Graham, T., Hegde, S., & Purushothaman, S. (1998). *Synth. Metals*, *92*, 47.
[4] Miyamae, T. & Nozoye, H. (2003). *Surface Science*, 532–535, 1045.
[5] Jian, C.L.J., Zhongfu, X., Gangjin, C., & Zhenzhong, W. (1998). *J. Electrostatics*, *44*, 61.
[6] Binnig, G., Quate, C. F., & Gerber, C. (1986). *Phys. Rev. Lett.*, *56*, 930.
[7] Perez, E. & Lang, J. (1999). *Macromolecules*, *32*, 1626.
[8] Saq'an, S., Ramadin, Y., Ahmad, M., Zihlif, A., Popovska-Pavlovska, F., & Trajkovska, A. (2001). *Polymer Testing*, *20*, 919.
[9] Perepechko, I.I. (1979). *An Introduction to Polymer Physics*, MIR: Moscow.
[10] Budaguan, B.G., Sherchenkov, A.A., Chern-omordic, V.D., Biriukov, A.V., & Ljung berg, L.Y. (1998). *J. Non-Cryst. Solids*, 227–230, 1123.
[11] Tareev, B. (1975). *Physics of Dielectric Materials*, MIR: Moscow.
[12] Bistac, S. & Schultz, J. (1997). *Progress in Organic Coatings*, *31*, 347.